3C16

Sr置換サイトによるNaTaO3光触媒の電子正孔結合の制御

（神戸大院・理）　○安 龍杰、Park Yohan、大西 洋

Electron-Hole Recombination Controlled by Sr Doping Sites in $NaTaO_3$ Photocatalyst

(Graduate School of Science, Kobe Univ.)　○Longjie An, Yohan Park, Hiroshi Onishi

Introduction

Metal (Sr, La or Ba) doped $NaTaO_3$ photocatalysts exhibited the world's record quantum efficiency (56% at maximum) of hydrogen evolution from water splitting upon UV irradiation.[1,2] Increased photocatalytic activity induced by metal dopants were attributed to restricted recombination of photoexcited electrons and holes,[3] however, the mechanism of how the recombination was restricted is remained uncertain.

Meanwhile, as a clue, particle surface was reconstructed to step structure when $NaTaO_3$ was doped with metals via solid-state method (SSM). In this study, Sr-doped $NaTaO_3$ photocatalysts were synthesized via SSM and their compositions and structures were determined expecting to explain the cause of the surface reconstruction.[4] Results of the characterization in combination of HF etching revealed that Sr^{2+} substituted Na^+ at A-sites and Ta^{5+} at B-sites, simultaneously, of perovskite-structured $NaTaO_3$ to form $NaTaO_3$-$Sr(Sr_{1/3}Ta_{2/3})O_3$ solid solutions with a Sr-rich shell covering a Sr-poor core.[5] Lattice mismatch between $NaTaO_3$ and $Sr(Sr_{1/3}Ta_{2/3})O_3$ induced particle surface to be reconstructed. At the same time, the electron-hole recombination was restricted drastically. To confirm the effect of Sr doping sites on the recombination rate, Sr doping at A-sites alone was tried and succeeded by hydrothermal method (HTM). Sr doping at A-sites did not restricted electron-hole recombination.

Experimental section

In SSM, Na_2CO_3, Ta_2O_5 and $SrCO_3$ were calcined in alumina crucible at 1173 K for 1 h, followed by calcination at 1423 K for 10 h. In HTM, Ta_2O_5 and $SrCO_3$ were heated in Teflon jar containing NaOH aqueous solution at 473 K for 20 h.[4] Surface or bulk compositions were quantified by XPS or EDX. Crystal structure or particle morphology and size were determined by XRD or SEM. Raman scattering was detected for observing change in lattice vibration. The steady-state population of photo-excited electrons not yet recombined with holes was evaluated from the change in IR absorbance induced by UV light irradiation. During process of etching, each photocatalyst (1 g) was stirred in HF solution (10 wt%, 3 ml) and then washed with water.[5]

Results and Discussion

Bulk Sr concentration was quantified as Sr/Ta molar ratio by EDX. Sr concentration in the products was almost the same as that in the starting materials. XRD patterns showed $NaTaO_3$ (NTO) and Sr-doped $NaTaO_3$ (Sr-NTO) of single perovskite-structured phases without an impurity phase. With increasing Sr concentration in Sr-NTOs prepared via SSM, XRD peaks broadened and shifted to low 2θ degrees, and gradually getting close to diffraction peaks of $Sr(Sr_{1/3}Ta_{2/3})O_3$[6] with Sr^{2+} occupying A- and B-sites simultaneously. The gradual shifts of XRD peaks suggest formation of solid-solution of $NaTaO_3$ and $Sr(Sr_{1/3}Ta_{2/3})O_3$. The ionic radii of Sr^{2+} and Na^+ are identical at 0.14 nm with a coordination number (CN) of 12, whereas Sr^{2+} (0.12 nm with a CN of 6) is twice larger than Ta^{5+} (0.06 nm with a CN of 6). Hence, the XRD peak shifts are naturally attributed to expansion of the unit cell of NTO by Sr doping at B-sites. At the same time, surface of photocatalysts particles was reconstructed to present 50-nm-wide terraces and 50-nm-high steps, according to scanning electron micrographs. The reconstruction is ascribed to lattice mismatch

across a Sr-rich shell and Sr-poor core of Sr-NTO. In HTM, XRD peak shifts and the surface reconstruction were absent to indicate Sr doping to A sites, not to B sites.

Different doping sites of Sr in NTO were further verified by Raman spectroscopy. **Figure 1** shows Raman spectra of NTO and Sr-NTO prepared via SSM and HTM. On SSM-prepared Sr-NTOs, two extra Raman bands appeared at 860 and 760 cm^{-1}, in addition to original lattice vibrational bands of NTO at 450, 500, and 620 cm^{-1}. These extra bands are assigned to breathing vibrations of BO_6 octahedra (A_{1g} symmetry) in the perovskite-structured lattice with B-sites partially replaced to be $A(B_{1-x}B'_x)O_3$. In fact, $Sr(Sr_{1/3}Ta_{2/3})O_3$ showed a strong A_{1g} band at 810 cm^{-1}. In an ideal perovskite, the BO_6 breathing vibration cannot contribute to Raman scattering due to symmetry restriction. Therefore, the extra bands indicate B-sites doping by Sr^{2+}. In HTM, again, no sign of B-sites doping was found.

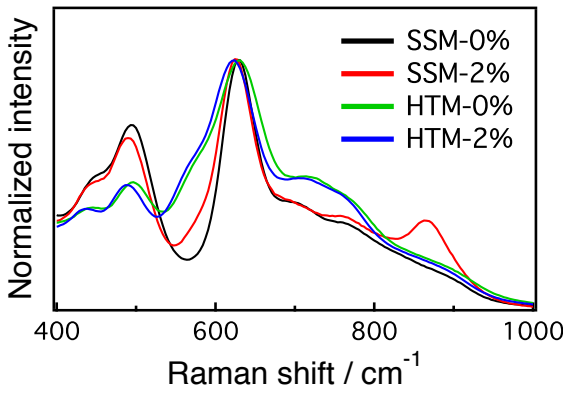

Figure 1. Raman spectra of NTO and 2% Sr-NTO synthesized via SSM or HTM.

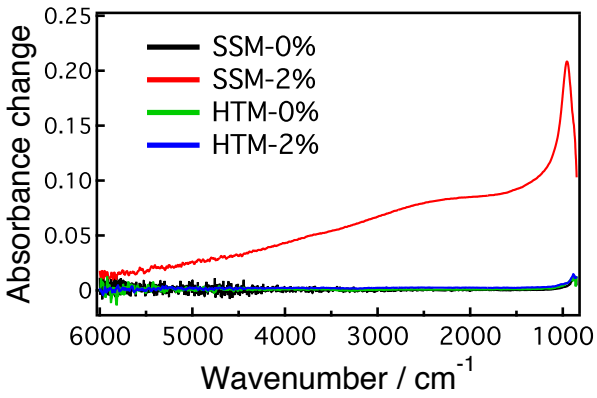

Figure 2. UV-induced IR absorbance change of NTO and 2% Sr-NTO synthesized via SSM or HTM.

To evaluate B-sites doping of Sr on the electron-hole recombination, population of photoexcited electrons were quantified by IR absorption in the presence of steady UV light irradiation. **Figure 2** shows IR absorbance change induced by UV light irradiation. On the SSM-prepared Sr-NTO, integrated absorbance change increased by 180 times. Restricted electron-hole recombination is ascribed to B-sites doping, since electron population was not enhanced in HTM-prepared Sr-NTO where Sr occupied A-sites.

Serious Sr segregation was detected by XPS on surface of SSM-prepared Sr-NTOs. Supported by reconstruction evidenced in the electron micrographs, we assume core-shell structure of the SSM-prepared Sr-NTOs. Sr-NTO particles were etched with a HF solution for revealing the role of the core and shell on electron-hole recombination. X-ray fluorescence and Raman results indicated that the core possessed Sr concentration gradient with more Sr in the outer core and less Sr in the inner core. Electron population was reduced gradually during etching on the core. On the other hand, removal of the shell induced electron population increased by 30%. This suggests that electrons were excited in the core and recombined in the shell.

Reference

(1) Kato, H.; Asakura, K.; Kudo, A. *J. AM. CHEM. SOC.* **2003**, *125*, 3082-3089.

(2) Iwase, A.; Kato, H.; Okutomi, H.; Kudo, A. *Chem. Lett.* **2004**, *33*, 1260-1261.

(3) Maruyama, M.; Iwase, A.; Kato, H.; Kudo, A.; Onishi, H. *J. Phys. Chem. C* **2009**, *113*, 13918-13923.

(4) An, L.; Onishi, H. *ACS Catal.*, **2015**, 5, 3196-3206.

(5) An, L.; Park, Y.; Sohn, Y.; Onishi, H. *J. Phys. Chem. C*, **2015**, *119*, 28440-28447.

(6) Yoshioka, K.; Petrykin, V.; Kakihana, M.; Kato, H.; Kudo, A. *J. Catal.* **2005**, *232*, 102−107.